Recording Fetal and Adult Magnetocardiograms Using High-Temperature Superconducting Quantum Interference Device Gradiometers

Yi Zhang, Norbert Wolters, Dieter Lomparski, Willi Zander, Marko Banzet, Hans-Joachim Krause, and Peter van Leeuwen

***Abstract*—In this paper, we analyze the influence of the superconducting quantum interference device (SQUID) gradiometer baseline on the recording of magnetocardiographic measurements. The magnetometers consist of high-temperature superconducting radio-frequency SQUIDs fabricated from YBaCuO thin films, and a substrate resonator which serves as tank circuit. The gradiometers are formed using two or three such magnetometers with individual readouts in electronic difference. We have compared the measurement results using a magnetometer and first- and second-order gradiometers with different baselines. In a standard magnetically shielded room, we found not only an increasing signal-to-noise ratio in adult magnetocardiographic measurements, but also a decreasing distortion of the magnetic field map with increasing baseline of the gradiometer. Using a first-order gradiometer with an ultralong baseline of 18 cm, we have successfully measured the heart signal of a fetus in real time.**

***Index Terms*—Biomagnetics, high-temperature superconductors, magnetocardiography, superconducting quantum interference device (SQUID) magnetometers.**

I. Introduction

RECENTLY, the interest on using magnetocardiography (MCG) as a diagnostic tool has increased [1]. Multichannel MCG systems based on low-temperature superconducting (LTS) superconducting quantum interference device (SQUID) are entering the medical market. In conventional LTS technology, one normally uses first-order axial gradiometers for suppression of external magnetic disturbances when recording MCGs inside a standard magnetically shielded room (MSR) and second-order gradiometers in an unshielded environment. For MCG evaluation, one typically records the MCG at 36 or more locations above the subjects chest and displays the result as a magnetic field map [2]. The data of the mapping can be further processed, e.g., by solving the inverse problem to determine the current distribution within the heart. It is expected that the cardiologists can use the information on the current distribution for diagnostic purposes, especially when analyzing the S-T regime (the repolarization time of the heart muscle which follows the QRS peak associated with the contraction of the ventricles) of the heart beat—in the case of ischemia [3].

MCG registration using high-temperature superconducting (HTS) SQUID magnetometers inside a MSR was already demonstrated ten years ago [4]–[6]. The HTS electronic gradiometer consists of SQUID magnetometers. A first-order axial gradiometer can be formed by subtracting the signals of a reference SQUID magnetometer from those of a sensing SQUID magnetometer [7], or by using a sensing SQUID and an orthogonal reference triple [8]. Second-order electronic gradiometers usually consist of three SQUID magnetometers in axial configuration with [9] or without mechanical balancing [10]. Such HTS gradiometers have been used to measure MCG signals without shielding.

If all magnetometers exhibit the same magnetic field noise $B_N(\mathrm{M})$, then the noise of the first-order gradiometer $B_N(\mathrm{G1}) = \sqrt{2}\ B_N(\mathrm{M})$ and the noise of the second-order gradiometer $B_N(\mathrm{G2}) = \sqrt{6}\ B_N(\mathrm{M})$. Therefore, the intrinsic noise of magnetometers is an important factor for gradiometer performance.

We have developed a radio-frequency (RF) SQUID magnetometer with an $SrTiO_3$substrate serving simultaneously as a tank circuit resonator [11]. This flux concentrator with an total pickup area of 10 $\times$ 10 mm is deposited directly on the resonator chip. The SQUID chip consists of a 5 $\times$ 5 mm substrate with a ditch, such that the epitaxial YBCO thin film forms a step edge Josephson Junction. The SQUID is structured to form our standard 3.5-mm-diameter washer layout with a 100 $\times$ 100 μm SQUID loop. The field to flux coefficient of the bare SQUID layout is about 10 nT/Φ_0, but with 10 $\times$ 10 mm flux concentrator in flip-chip configuration it improves to 3.2 nT/Φ_0. In this configuration, the working point of the RF SQUID is somewhat stabilized, thus, reducing the low-frequency noise [12].

In this paper, we will discuss the influence of the gradiometer baseline length on the MCG measurement using software gradiometry. For hardware gradiometry, this issue has been examined previously [13]. Also, we report the first recording of the heart signal of an unborn baby (fetus) using an HTS RF SQUID first-order gradiometer.

II. System Configurations

In the following MCG measurements, we used two different systems.

Manuscript received September 25, 2003. This paper was recommended by Associate Editor N. F. Pedersen.

Y. Zhang, N. Wolters, D. Lomparski, W. Zander, M. Banzet, and H.-J. Krause are with the Institute of Thin Films and Interfaces (ISG-2), 52425 Jülich, Germany (e-mail: y.zhang@fz-juelich.de).

P. van Leeuwen is with Entwicklungs und Forschungszentrum für MikroTherapie gGmbH (EFMT), 44799 Bochum, Germany.

Digital Object Identifier 10.1109/TASC.2003.820505

System 1: Three magnetometers described above were arranged in axial configuration. The white magnetic field noise of each was determined to be about 30 $\mathrm{fT}/\sqrt{\mathrm{Hz}}$ in shielding. The baseline length was 9 cm. The sensing magnetometer A was placed at the bottom of the dewar. The reference magnetometer B was situated in the middle, reference magnetometer C was located at the top. We analyzed four configurations:

M(A)	only using sensing magnetometer A;
$\mathrm{G1(A-B)}$	first-order gradiometer with a baseline of 9 cm;
$\mathrm{G1(A-C)}$	first-order gradiometer with a baseline of 18 cm;
$\mathrm{G2(A-2B+C)}$	second-order gradiometer with a baseline of 9 cm.

The configuration could be changed *in situ* during the measurement.

System 2: A first-order axial gradiometer with variable baseline. The baseline could be changed from 2 to 18 cm *ex situ*. The pickup area was increased by using an additional flux concentrator, 1 inch in diameter, deposited on $LaAlO_3$. An 8-mm hole was drilled in the center of the flux concentrator chip. The concentrator was placed at the same level as the SQUID chip.

Because of the larger pickup area, the field to flux coefficient was reduced to 1.6 nT/Φ_0. The flux noise remained unchanged after introducing the concentrator. Therefore, the magnetic field sensitivity of the magnetometer was improved to 15 $\mathrm{fT}/\sqrt{\mathrm{Hz}}$.

III. Adult MCG Measurements

Using System 1 in a standard MSR, we conducted MCG measurements on two adult subjects, Person X (male, 28 years, 175 cm tall, weight 68 kg) and Person Y (male, 54 years, 172 cm tall, weight 80 kg). The mapping points were labeled consecutively A–F (cranial–caudal) and 1–6 (left–right). The grid line A intersected the sternal notch, with the notch half way between A3 and A4. The measurement grid period was 3.5 cm in both directions. In all measurements, a two-lead electrocardiogram was also recorded and used to trigger the averaging process.

Fig. 1 shows the normalized measurement data (QRS peak-to-peak value) of the first-order gradiometers $\mathrm{G1(A-B)}$, $\mathrm{G1(A-C)}$, and the second-order gradiometer $\mathrm{G2(A-2B+C)}$, normalized to the level of the QRS peak of the magnetometer recording with sensor M(A) at the same point.

The normalized data show that the QRS field strength is reduced and varies from point-to-point of the grid. The reduction depends not only on the baseline length [compare Fig. 1(a) and (b)], gradient order with a same baseline length [compare Fig. 1(a) and (c)], but also on the patient [compare Fig. 1(c) and (d)]. Table I shows the mean values, their standard deviations, and extremes values of the three gradiometer recordings relative to the magnetometer measurement. For both subjects X and Y, the normalized QRS peak value is shown averaged over all 36 grid points. Two tendencies can be clearly observed: 1) for the first-order gradiometer, the longer baseline results in lower variance in the mapping data (as compared to magnetometer mapping, which is assumed as reference) than the shorter baseline; 2) with the same baseline, the first-order gradiometer recording results in less distortion than the second-order gradiometer.

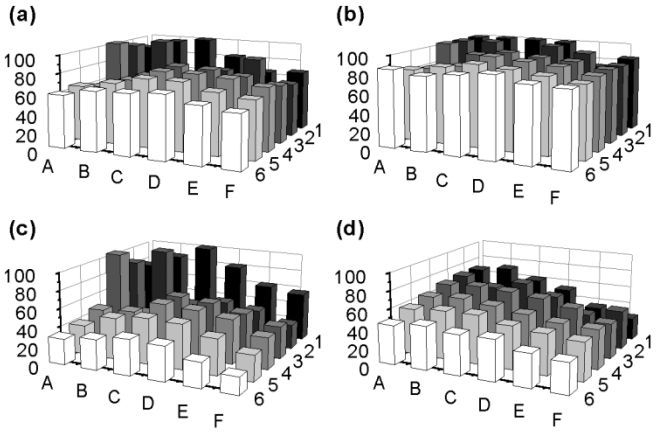

Fig. 1. QRS peak-to-peak value (taken from average over 20 s) at the grid positions for all three gradiometer configurations, normalized to the value of magnetometer mapping. (a) $\mathrm{G1(A-B)}$ of Person X. (b) $\mathrm{G1(A-C)}$ of Person X. (c) $\mathrm{G2(A-2B+C)}$ of Person X. (d) $\mathrm{G2(A-2B+C)}$ of Person Y.

TABLE I
Statistical Data on the MCG Measurements With the Three Gradiometer Configurations, Normalized to the Magnetometer Measurement

	Normalized Average		Standard Deviation		Maximum Value		Minimum Value	
Subject	*X*	*Y*	*X*	*Y*	*X*	*Y*	*X*	*Y*
A – B	*72*	*69*	*12*	*7.7*	*100*	*84*	*50*	*52*
A – C	*88*	*87*	*8.7*	*5.7*	*100*	*100*	*62*	*76*
A – 2B + C	*51*	*51*	*21*	*10*	*100*	*70*	*19*	*25*

The values are in %.

A current density reconstruction of the repolarization period (ST-T) might be helpful in determining the distorting influence of the used gradiometer configuration. By lack of appropriate software tools, we were not able to perform such an analysis. However, Burghoff *et al.* found that the isocontour maps recorded with different LTS multichannel first-order gradiometer systems are different [14].

It is true that cardiac depolarization and repolarization is a complex process and that the spatial variation of the R and S peaks are different. This may lead to incongruities in the normalization of the peak-to-peak values. Nonetheless, we do not expect these to be very large and feel that the normalization is appropriate to permit the comparison of different gradiometer configurations.

Using our System 2, we varied the baseline of the first-order gradiometer from 2 to 18 cm in steps of 4 cm. We observed the MCG signal of Person Y at five selected grid points with different baseline lengths of the gradiometer. The four corners of our mapping area, A1, A6, F1, and F6, were chosen as four measurement points. Additionally, point D4 was chosen since at that point, the recorded MCG signal is usually strongest.

Fig. 2 displays the dependence of the normalized QRS signal recorded at these points as a function of baseline. We observe that signal strength at points A1, A6, and D4 increases relatively slowly if the baseline is larger than 10 cm, but the signal at points F1 and F6 is very strongly dependent on baseline even for large baselines. From Fig. 2, one may conclude that the conventional baseline length of 5–7 cm is too short as the baseline unduly reduces MCG signal strength (see, e.g., points F1 and F6).

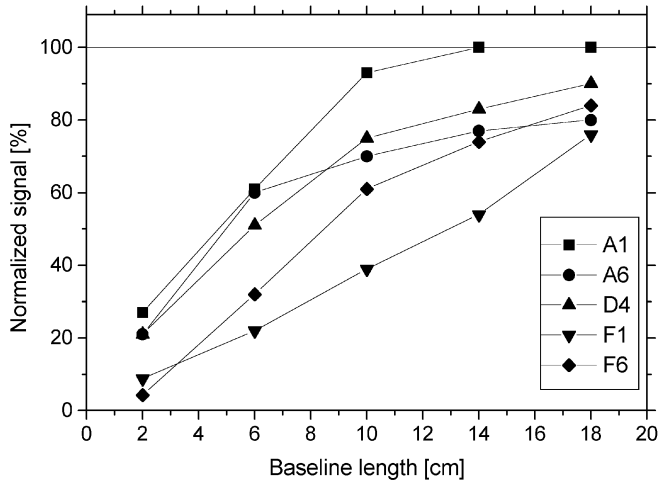

Fig. 2. Normalized QRS peak values of Person Y, recorded at five selected grid points, as a function of the baseline lengths of the first-order gradiometer with a pickup area of 1 in.

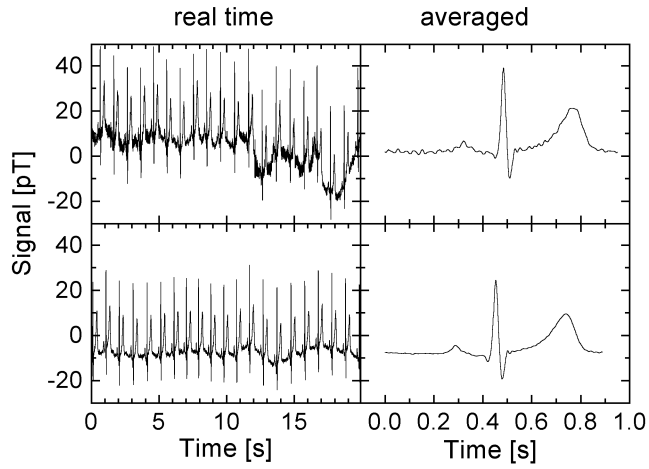

Fig. 3. Real-time and averaged MCG signals in our MSR recorded using System 2 (upper panel, magnetometer; lower panel, gradiometer with an 18-cm baseline).

Fig. 3 demonstrates two real-time MCG measurements using System 2, one using the first-order gradiometer with an 18-cm baseline (Fig. 3, lower panel), the other with the magnetometer (upper panel). Both measurements were recorded in our MSR. Compared to the magnetometer, the first-order gradiometer showed better SNR in real time (see Fig. 3, left panels) and in the averaged data (Fig. 3, right panels). The magnetometer signal exhibited more disturbances than the gradiometer, not only the power line noise, but also in low frequency regime.

We found that in our MSR, the gradiometer noise is not significantly dependent on the baseline. Thus, gradient noise is not dominant. If the noise of both magnetometers is equal, the noise will be $\sqrt{2}$ times higher for the first-order gradiometer compared to the magnetometer noise. The gradiometer noise measured in our MSR fits the expected theoretical values very well, at least for frequencies >3 Hz.

We denote the MCG signal with "s" and the intrinsic magnetometer noise amplitude with "n." Thus, the highest reachable SNR is s/n. For an ideal first-order gradiometer consisting of two SQUID magnetometers, the measured signal s should not be reduced, but the noise would be $\sqrt{2}\ n$. Consequently, the largest SNR would be 0.71 s/n. In Table II, the averaged SNR data are listed and compared to the ideal SNR values of the gradiometers. From Table II, we can see that our first-order gradiometer $\mathrm{G1(A-C)}$ with an 18-cm baseline performs well for MCG measurements. The possibility to form gradiometers with ultralong baselines is a main advantage of electronic gradiometers, as compared to the LTS pickup antenna technology.

TABLE II
AVERAGED AND IDEAL SNRS OF DIFFERENT GRADIOMETER CONFIGURATIONS

	Signal [s]	*Noise [n]*	*SNR [s/n]*
A – B	*0.7*	*1.4*	*0.50*
A – C	*0.88*	*1.4*	*0.62*
*Ideal 1st order gradiometer**	*1*	$\sqrt{2} \approx 1.41$	$1/\sqrt{2} \approx 0.71$
A – 2B + C	0.51	2.5	0.20
Ideal 2nd order gradiometer*	1	$\sqrt{6} \approx 2.45$	$1/\sqrt{6} \approx 0.41$

* the theoretical values are listed.

IV. FETAL MCG MEASUREMENTS

Of course, the choice of the baseline is also dependent on the measurement object. For example, the volume of a fetal heart is much smaller than an adult heart. Therefore, the magnetic signal reduces more quickly with distance between heart and SQUID sensor. For a fetal MCG recording, our gradiometer with an 18-cm baseline is more close to ideal. We have conducted fetal MCG measurements in a standard MSR (Vakuumschmelze AK3b, Hanau, Germany) with both our HTS and an LTS system. The latter was a 61-channel biomagnetometer specially designed for fetal measurements (4D-Neuroimaging Magnes 1300C [15]) pickup area and first-order electronic gradiometers with an 18-cm baseline. Fetal MCG data have been recorded routinely with this system since 1997 [16]. The HTS recordings were done with System 1, $\mathrm{G1(A-C)}$ configuration, and with System 2, both first-order gradiometers with an 18-cm baseline. We performed measurements on two fetuses, one in the 37th week and one in the 38th week of gestation. First, the LTS system was placed over the maternal abdomen and data were collected for 5 min. The location of the maximal fetal QRS amplitude over the maternal abdomen was determined by examining the data in all 61 channels. The HTS sensor was then positioned above this site and a further 5 min of data were obtained. Using the system $\mathrm{G1(A-C)}$, we measured the heart signal of the fetus in the 37th week. The measured real-time trace [Fig. 4(a)] exhibits both the fetal heart signal and maternal heart signal. The SQUID gradiometer system noise was about <2 pT peak-to-peak with a video bandwidth of 90 Hz. The QRS peak of the fetal heart beat was about 4 pT, yielding an SNR of about two for the real-time data. The standard procedure to enhance the SNR, which is usually applied to the LTS measurements, was also used here: By correlation analysis, the maternal heart beats were identified, averaged, and subtracted. In the resulting signal, all fetal beats were identified and beats which correlated well with the fetal QRS template were averaged [$n > 350$, see Fig. 4(b)].

In order to further enhance the SNR ratio, we used System 2 with 1-in flux focusers because its system noise was only about 1 pT peak-to-peak (with a video bandwidth of 90 Hz). Fig. 5

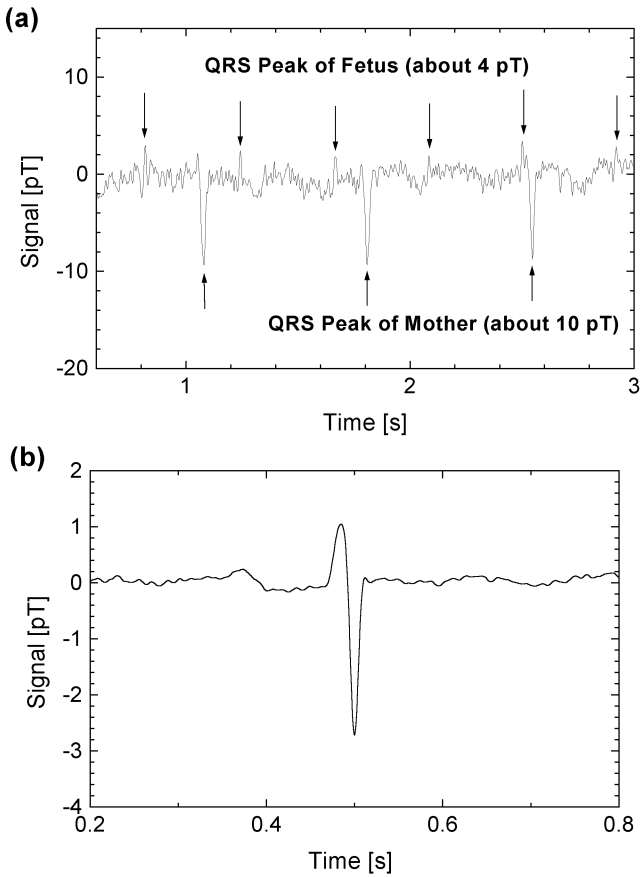

Fig. 4. (a) Measured time traces of a fetus at 37th week of gestation, recorded using $G1(A-C)$. (b) Averaged fetal heart signal.

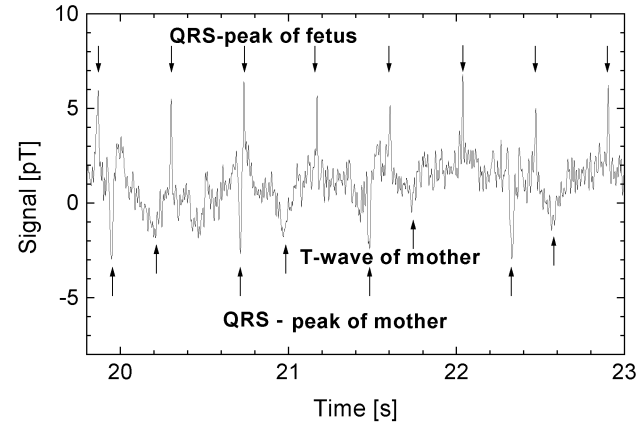

Fig. 5. Measured real-time traces of fetal at 38th week of gestation, recorded using System 2 with an 18-cm baseline.

shows the real-time trace acquired from a fetus at 38th week of gestation. The fetal heart beat was about 5 pT and the SNR was about five in real time. The fetal signal was also measured with the LTS system which exhibited a noise of about 250 fT peak-to-peak with the same pickup area, video bandwidth, and baseline.

It is, of course, true that biological noise is present in any cardiographic measurement. However, the results presented in Table II show no great discrepency between theoretical and measured values indicating that biological noise probably played a lesser role. But one may further expect that, compared to LTS measurements, biological noise will not be so predominant in HTS measurements because of the higher system noise.

V. Conclusion

We have analyzed MCG mappings of adult subjects performed with HTS SQUID magnetometer and different gradiometer configurations. We found that gradiometer mappings yield distorted magnetic field maps compared to magnetometer mappings. The distortion is weaker for first-order gradiometer as compared to second-order, and for long baselines. Using a first-order gradiometer with ultralong baseline of 18 cm in standard MSR, we measured fetal MCG signals, reaching an SNR of up to five in real time. These measurements represent the first demonstration that HTS SQUIDs may be practically applied to fetal MCG.

Acknowledgment

The authors would like to thank A. I. Braginski and M. Mück for their critical remarks, suggestions, and help in preparation of the manuscript of this paper.

References

[1] H. Nowak, J. Haueisen, F. Gießler, and R. Huonker, Eds., *Proc. 13th Int. Conf. Biomagnetism*. Jena, Germany: VDE Verlag, 2002.

[2] S. N. Erné, R. R. Fenici, H.-D. Hahlbohm, J. Korsukewitz, H. P. Lehmann, and Y. Uchikawa, *Biomagnetism: Application and Theory*, H. Weinberg, G. Stroink, and T. Katila, Eds. New York: Pergamon, 1984, pp. 132–142.

[3] G. Stroink, *Recent Advances in Biomagnetism*, T. Yoshimoto, M. Kotani, S. Kuriki, H. Karibe, and N. Nakasato, Eds. Sendai, Japan: Tohoku Univ. Press, 1999, pp. 982–985.

[4] A. H. Miklich, J. J. Kingston, F. C. Wellstood, J. Clarke, M. S. Colclough, K. Char, and G. Zaharchuk, "Thin-film YBCO magnetometer," *Nature*, vol. 352, pp. 482–484, 1991.

[5] Y. Zhang, Y. Tavrin, M. Mück, A. I. Braginski, C. Heiden, T. Elbert, and S. Hampson, "High temperature rf SQUIDs for biomedical applications," *Clinical Physics and Physiological Measurement*, vol. 14, pp. 113–116, 1993.

[6] F. Ludwig, E. Dantsker, D. Koelle, R. Kleiner, A. H. Miklich, and J. Clarke, "Multilayer magnetometers based on high-T_c SQUIDs," *Appl. Supercond.*, vol. 3, pp. 383–398, 1995.

[7] Y. Tavrin, Y. Zhang, M. Mück, A. I. Braginski, and C. Heiden, "$YBa_2Cu_3O_7$ thin film SQUID gradiometer for biomagnetic measurements," *Appl. Phys. Lett.*, vol. 62, no. 15, pp. 1824–1826, 1993.

[8] D. F. He, H.-J. Krause, Y. Zhang, M. Bick, H. Soltner, N. Wolters, W. Wolf, and H. Bousack, " HTS SQUID magnetometer with SQUID vector reference for operation in unshielded environment," *IEEE Trans. Appl. Superconduct.*, vol. 9, pp. 3684–3687, June 1999.

[9] Y. Tavrin, Y. Zhang, W. Wolf, and A. I. Braginski, "A second-order SQUID gradiometer operating at 77 K," *Supercond. Sci. Technol.*, vol. 7, pp. 265–267, 1994.

[10] Y. Zhang, G. Panaitov, S. G. Wang, N. Wolters, R. Otto, J. Schubert, W. Zander, H.-J. Krause, H. Soltner, H. Bousack, and A. I. Braginski, "Second-order, high-temperature SQUID gradiometer for magnetocardiography in unshielded environment," *Appl. Phys. Lett.*, vol. 76, pp. 906–908, 2000.

[11] Y. Zhang, J. Schubert, N. Wolters, M. Banzet, W. Zander, and H.-J. Krause, "Substrate resonator for HTS rf SQUID operation," *Physica C*, vol. 372–376, pp. 282–285, 2002.

[12] Y. Zhang, N. Wolters, J. Schubert, D. Lomparski, M. Banzet, G. Panaitov, H.-J. Krause, M. Mück, and A. I. Braginski, "HTS SQUID gradiometer using substrate resonators operating in unshielded environment—A portable MCG system," *IEEE Trans. Appl. Superconduct.*, vol. 13, pp. 389–392, June 2003.

[13] P. Carelli, I. Modena, and G. L. Romani, "Detection coils," in *Biomagnetism, an Interdisciplinary Approach*, S. J. Williamson, G. L. Romani, L. Kaufman, and I. Modena, Eds. New York: Plenum, 1982, pp. 85–99.

[14] M. Burghoff, J. Nenonen, L. Trahms, and T. Katila, "Conversion of magnetocardiographic recordings between two different multichannel SQUID devices," *IEEE Trans. Biomed. Eng.*, vol. 47, pp. 869–875, July 2000.
[15] P. van Leeuwen, C. Haupt, C. Hoormann, B. Hailer, B. M. Mackert, and G. Stroink, *Recent Advances in Biomagnetism*, T. Yoshimoto, M. Kotani, S. Kuriki, H. Karibe, and N. Nakasato, Eds. Sendai, Japan: Tohoku Univ. Press, 1999, pp. 89–92.
[16] P. van Leeuwen, D. Geue, S. Lange, D. Cysarz, H. Bettermann, and D. Groenemeyer, "Is there evidence of fetal-maternal heart rate synchronization?," *BMC Physiol.*, vol. 3, no. 1, p. 2, 2003.

Yi Zhang was born in Shanghai, China, in 1948. He received the Diploma and Ph.D. degrees from the Justus Liebig University, Giessen, Germany, in 1987 and 1990, respectively.

He joined the Research Center Jülich, Jülich, Germany, in 1990, dedicating his work to the development and application of HTS RF-SQUIDs. He developed SQUID sensors and readout electronics for numerous specialized applications. In 1995, he received the title of Professor from the University of Beijing, China. In 2001, he spent four months as a guest scientist at the University of California, Berkeley, in Prof. John Clarke's group, working on the novel superconductor magnesiumdiboride and developing the first MgB2 SQUID. Currently, he focuses on the development of HTS SQUID systems for magnetocardiography.

Norbert Wolters was born in Aachen, Germany, in 1961.

He joined the Research Center Jülich, Jülich, Germany, in 1979, as an apprentice in information electronics and became a full employee in 1983, working on the development of electronics for the spallation neutron source. In 1987, he finished his vocational training as an Electronics Engineer and became a team member of the Electronics Department, of the Institute of Thin Films and Ion Technology. His expertise lies in the field of general electronics development, layout, and setup, as well as micro controller programming. He is an expert on RF SQUID readout electronics and computerized system control.

Dieter Lomparski was born in Heinsberg, Germany, in 1963. After an apprenticeship as a toolmaker, he studied applied physics and received the Applied Physics Engineer diploma from the Aachen University of Applied Sciences, Aachen, Germany, in 1992.

He joined the SQUID Application Department, Research Center Jülich, Jülich, Germany, in 1993, working on SQUID system technology for industrial magnetometry applications. His expertise covers the field of system engineering for sensitive magnetic detection, electromagnetic interference suppression, low magnetic noise scanning devices, data acquisition, and computerized system control for applications in electromagnetic nondestructive evaluation of materials and human magnetocardiography.

Willi Zander was born in Aldenhoven, Germany, in 1952.

He joined the Research Center Jülich, Jülich, Germany, in 1968, as a Mechanic Apprentice. In 1977, he concluded his vocational training as a Mechanical Engineer. His expertise lies in the field of low-temperature physics, cryostat technology, vacuum technology, and construction and setup of laser ablation systems. In 1997, he co-founded the Jülich SQUID Company as a spin-off, manufacturing and distributing SQUID components and systems as well as thin film deposition systems. Since 2001, he has led the company as Chief Executive Officer.

Marko Banzet was born in Dinslaken, Germany, in 1973.

He joined the Research Center Jülich, Jülich, Germany, in 1989, as a Physics Laboratory Assistant. Since 1992, he works as a Technician in the field of superconductivity, thin-film deposition, ion beam etching, lithographic structuring, and clean room technology. Currently, he participates in vocational training as an Information Technology Engineer.

Hans-Joachim Krause was born in Hamburg, Germany, in 1963. He studied physics and mathematics in Braunschweig and Aachen, Germany, and received the Diploma degree in physics in 1990. He received the Ph.D. degree from the Technical University Aachen, Aachen, Germany, in 1993.

He joined the Research Center Jülich, Jülich, Germany, in 1990. From 1990 to 1993, he developed tunable high power laser systems for nonlinear optical spectroscopy at interfaces. Since then, he has been working on the application-oriented development of HTS SQUID systems at the Research Center Jülich, mainly for industrial use of SQUIDs, e.g., in nondestructive evaluation of aircraft parts. Currently, he leads the SQUID Application Group, focusing on the detection of magnetic nanoparticles for cell sorting and immunoassay applications.

Peter van Leeuwen was born in The Hague, The Netherlands, in 1949. He studied mathematics and pedagogy in Montreal, QC, Canada, and received the Bachelor of Education degree in 1971. He received the Ph.D. degree in medical science from the University of Witten/Herdecke, Witten, Germany in 1989.

From 1980 to 1991, he worked as a Researcher in the community hospital in Herdecke, Germany, the main emphasis being on the improvement of noninvasive diagnostic procedures in cardiology such as heart rate variability analysis. Since 1992, he has led the Department of Biomagnetism in the Research and Development Center for Microtherapy in Bochum, Germany. The main topics of his work focus on the development of diagnostic procedures in adult and fetal cardiology using biomagnetic techniques.